Received 18 February; accepted 23 March 2003; doi:10.1038/nature02516.

1. Kende, H. Ethylene biosynthesis. *Annu. Rev. Plant Physiol. Plant Mol. Biol.* **44,** 283–307 (1993).
2. Wang, K. L., Li, H. & Ecker, J. R. Ethylene biosynthesis and signaling networks. *Plant Cell* **14,** S131–S151 (2002).
3. Vogel, J. P. *et al.* Recessive and dominant mutations in the ethylene biosynthetic gene *ACS5* of *Arabidopsis* confer cytokinin insensitivity and ethylene overproduction, respectively. *Proc. Natl Acad. Sci. USA* **95,** 4766–4771 (1998).
4. Chae, H. S., Faure, F. & Kieber, J. J. The *eto1*, *eto2*, and *eto3* mutations and cytokinin treatment increase ethylene biosynthesis in *Arabidopsis* by increasing the stability of ACS protein. *Plant Cell* **15,** 545–559 (2003).
5. Yang, S. F. & Hoffman, N. E. Ethylene biosynthesis and its regulation in higher plants. *Annu. Rev. Plant Physiol. Plant Mol. Biol.* **35,** 155–189 (1984).
6. Bleecker, A. B. & Kende, H. Ethylene: a gaseous signal molecule in plants. *Annu. Rev. Cell Dev. Biol.* **16,** 1–18 (2000).
7. Spanu, P. *et al.* The apparent turnover of 1-aminocyclopropane-1-carboxylate synthase in tomato cells is regulated by protein phosphorylation and dephosphorylation. *Plant Physiol.* **106,** 529–535 (1994).
8. Guzman, P. & Ecker, J. R. Exploiting the triple response of *Arabidopsis* to identify ethylene-related mutants. *Plant Cell* **2,** 513–523 (1990).
9. Roman, G. *et al.* Genetic analysis of ethylene signal transduction in *Arabidopsis thaliana*: five novel mutant loci integrated into a stress response pathway. *Genetics* **139,** 1393–1409 (1995).
10. Kieber, J. J. *et al.* CTR1, a negative regulator of the ethylene response pathway in *Arabidopsis*, encodes a member of the raf family of protein kinases. *Cell* **72,** 427–441 (1993).
11. D'Andrea, L. D. & Regan, L. TPR proteins: the versatile helix. *Trends Biochem.* **28,** 655–662 (2003).
12. Collins, T., Stone, J. R. & Williams, A. J. All in the family: the BTB/POZ, KRAB, and SCAN domains. *Mol. Cell. Biol.* **21,** 3609–3615 (2001).
13. Lizada, M. C. & Yang, S. F. A simple and sensitive assay for 1-aminocyclopropane-1-carboxylic acid. *Anal. Biochem.* **100,** 140–145 (1979).
14. Tarun, A. S., Lee, J. S. & Theologis, A. Random mutagenesis of 1-aminocyclopropane-1-carboxylate synthase: a key enzyme in ethylene biosynthesis. *Proc. Natl Acad. Sci. USA* **95,** 9796–9801 (1998).
15. Tsuchisaka, A. & Theologis, A. Heterodimeric interactions among the 1-amino-cyclopropane-1-carboxylate synthase polypeptides encoded by the *Arabidopsis* gene family. *Proc. Natl Acad. Sci. USA* **101,** 2275–2280 (2004).
16. Hershko, A. & Ciechanover, A. The ubiquitin system. *Annu. Rev. Biochem.* **67,** 425–479 (1998).
17. Hellmann, H. & Estelle, M. Plant development: regulation by protein degradation. *Science* **297,** 793–797 (2002).
18. Xu, L. *et al.* BTB proteins are substrate-specific adaptors in an SCF-like modular ubiquitin ligase containing CUL-3. *Nature* **425,** 316–321 (2003).
19. Pintard, L. *et al.* The BTB protein MEL-26 is a substrate-specific adaptor of the CUL-3 ubiquitin-ligase. *Nature* **425,** 311–316 (2003).
20. Geyer, R. *et al.* BTB/POZ domain proteins are putative substrate adaptors for cullin 3 ubiquitin ligases. *Mol. Cell* **12,** 783–790 (2003).
21. Furukawa, M. *et al.* Targeting of protein ubiquitination by BTB-Cullin 3-Roc1 ubiquitin ligases. *Nature Cell Biol.* **5,** 1001–1007 (2003).
22. Kobe, B. & Kemp, B. E. Active site-directed protein regulation. *Nature* **402,** 373–376 (1999).
23. Capitani, G. *et al.* Structure of 1-aminocyclopropane-1-carboxylate synthase, a key enzyme in the biosynthesis of the plant hormone ethylene. *J. Mol. Biol.* **294,** 745–756 (1999).
24. Tarun, A. S. & Theologis, A. Complementation analysis of mutants of 1-aminocyclopropane-1-carboxylate synthase reveals the enzyme is a dimer with shared active sites. *J. Biol. Chem.* **273,** 12509–12514 (1998).
25. Potuschak, T. *et al.* EIN3-dependent regulation of plant ethylene hormone signaling by two *Arabidopsis* F box proteins: EBF1 and EBF2. *Cell* **115,** 679–689 (2003).
26. Guo, H. & Ecker, J. R. Plant responses to ethylene gas are mediated by $SC^{EBF1/EBF2}$-dependent proteolysis of EIN3 transcription factor. *Cell* **115,** 667–677 (2003).
27. Tatsuki, M. & Mori, H. Phosphorylation of tomato 1-aminocyclopropane-1-carboxylic acid synthase, LE-ACS2, at the C-terminal region. *J. Biol. Chem.* **276,** 28051–28057 (2001).
28. Yamagami, T. *et al.* Biochemical diversity among the 1-amino-cyclopropane-1-carboxylate synthase isozymes encoded by the *Arabidopsis* gene family. *J. Biol. Chem.* **278,** 49102–49112 (2003).
29. Yamada, K. *et al.* Empirical analysis of transcriptional activity in the *Arabidopsis* genome. *Science* **302,** 842–846 (2003).
30. Liu, Q. *et al.* The univector plasmid-fusion system, a method for rapid construction of recombinant DNA without restriction enzymes. *Curr. Biol.* **8,** 1300–1309 (1998).

Supplementary Information accompanies the paper on **www.nature.com/nature**.

Acknowledgements We thank members of the Ecker laboratory for stimulating discussion; J. Chory, J. Umen, S. Liljegren and J. Borevitz for critical reading of the manuscript; T. Hirayama for providing F_2 seeds of the mapping cross; and A. Theologis for the JAde6 strain. K.L.-C.W. acknowledges support from a fellowship from the Pioneer Foundation. H.Y. acknowledges support from a long-term fellowship from the Japanese Science and Technology Agency. C.L. acknowledges support from a long-term fellowship from the Human Frontier Science Program. This research was supported by grants from the Department of Energy and the National Science Foundation to J.R.E.

Competing interests statement The authors declare that they have no competing financial interests.

Correspondence and requests for materials should be addressed to J.R.E. (ecker@salk.edu). The GenBank accession numbers for *ETO1*, *EOL1* and *EOL2* cDNA are AY572791, AY572792 and AY572793, respectively.

Cadherin 23 is a component of the tip link in hair-cell stereocilia

Jan Siemens[1], Concepcion Lillo[2], Rachel A. Dumont[3], Anna Reynolds[1], David S. Williams[2], Peter G. Gillespie[3] & Ulrich Müller[1]

[1]*The Scripps Research Institute, Department of Cell Biology, Institute for Childhood and Neglected Disease, La Jolla, California 92037, USA*
[2]*Department of Pharmacology and Neuroscience, School of Medicine, University of California at San Diego, La Jolla, California 92093-0912, USA*
[3]*Oregon Hearing Research Center & Vollum Institute, Oregon Health & Science University, Portland, Oregon 97239, USA*

Mechanoelectrical transduction, the conversion of mechanical force into electrochemical signals, underlies a range of sensory phenomena, including touch, hearing and balance. Hair cells of the vertebrate inner ear are specialized mechanosensors that transduce mechanical forces arising from sound waves and head movement to provide our senses of hearing and balance[1,2]; however, the mechanotransduction channel of hair cells and the molecules that regulate channel activity have remained elusive. One molecule that might participate in mechanoelectrical transduction is cadherin 23 (CDH23), as mutations in its gene cause deafness and age-related hearing loss[3–6]. Furthermore, CDH23 is large enough to be the tip link, the extracellular filament proposed to gate the mechanotransduction channel[7]. Here we show that antibodies against CDH23 label the tip link, and that CDH23 has biochemical properties similar to those of the tip link. Moreover, CDH23 forms a complex with myosin-1c, the only known component of the mechanotransduction apparatus[8], suggesting that CDH23 and myosin-1c cooperate to regulate the activity of mechanically gated ion channels in hair cells.

The mechanically sensitive organelle of the hair cell, the hair bundle, contains dozens of actin-rich stereocilia and a single microtubule-based kinocilium (Fig. 1a). Mechanotransduction channels are located towards stereociliary tips and open or close on deflection of the stereocilia[1–2]. Excitatory stimuli stretch a gating spring, an elastic element that gates the mechanotransduction channels[9]. Of the extracellular filaments that interconnect stereocilia or stereocilia and the kinocilium, only the 150–200-nm tip link is correctly positioned to control opening of mechanotransduction channels[7,10]. The molecular composition of the tip link is not known, but it has similarities with links between kinocilia and stereocilia; both structures are recognized by an antibody against an unknown protein termed the tip link antigen[11]. The tip link also shares features with cadherins. Not only does the tip link mediate adhesive interactions between adjacent plasma membranes, but Ca^{2+} chelating agents disrupt the tip link[10] and cadherin adhesive function[12]. Because single cadherin domains span approximately 4 nm[13], homophilically interacting CDH23 molecules, with 27 cadherin domains each, could span >200 nm.

Two alternatively spliced CDH23 isoforms differing with respect to the inclusion of exon 68, encoding part of the intracellular CDH23 domain, have been described[3,5,14] (Fig. 1b). Using polymerase chain reaction with reverse transcription (RT–PCR), we detected messenger RNAs encoding CDH23(+68) and CDH23(−68) in inner ears of adult mice; CDH23(+68) was prominent in the inner ear but was not detected in other tissues (Fig. 1c and data not shown). To localize CDH23 protein, we used an antibody (CDH23*cyto) that recognizes the cytoplasmic domain of both isoforms, and another antibody (CDH23*68) that is specific for CDH23(+68) (Supplementary Fig. 1). At postnatal days 0 and 5 (P0 and P5, respectively), when cochlear hair cells are immature and contain a kinocilium, CDH23*cyto detected CDH23 in the developing hair bundle and in Reissner's membrane (Fig. 1e, g, h). By

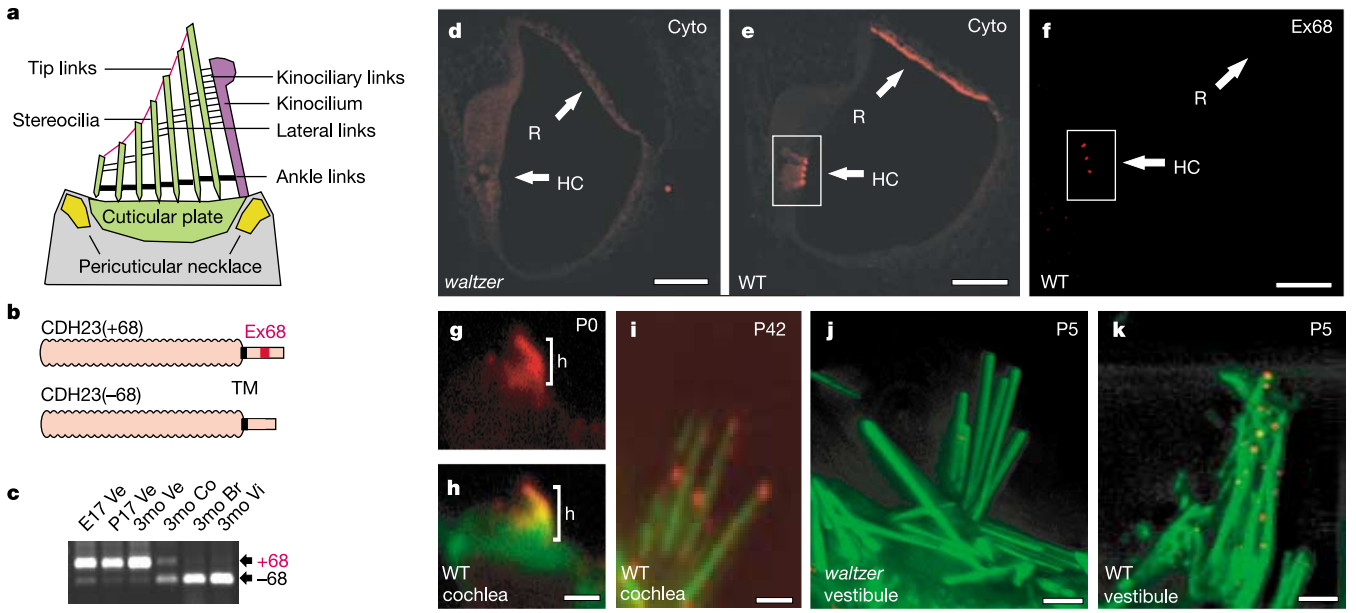

Figure 1 CDH23 expression in mouse inner ears. **a**, Stereocilia are connected through tip, lateral and ankle links, and to the kinocilium through kinocilia links. **b**, CDH23 protein. Exon 68 is present only in CDH23(+68). TM, transmembrane domain. **c**, Analysis of CDH23 expression in the vestibule (VE), cochlea (Co), brain (Br) and vibrissae (Vi). E17, embryonic day 17; P17, postnatal day 17; 3mo, 3 months. **d**–**f**, Section of a P5 cochlea. **d**, **e**, CDH23*cyto (red) stained hair cells (HC) and Reissner's membrane (R) in wild-type (WT) but not in *Cdh23*-deficient *waltzer* mice. **f**, CDH23*68 stained hair bundles only. **g**, **h**, CDH23 (red) in immature P0 cochlear hair cells was distributed throughout the hair bundle (h) (green, phalloidin). **i**–**k,** CDH23 in mature hair cells was confined to stereociliary tips, but was absent in *waltzer* mice. Scale bars: **d**–**f**, 40 μm; **g**–**k**, 1.25 μm.

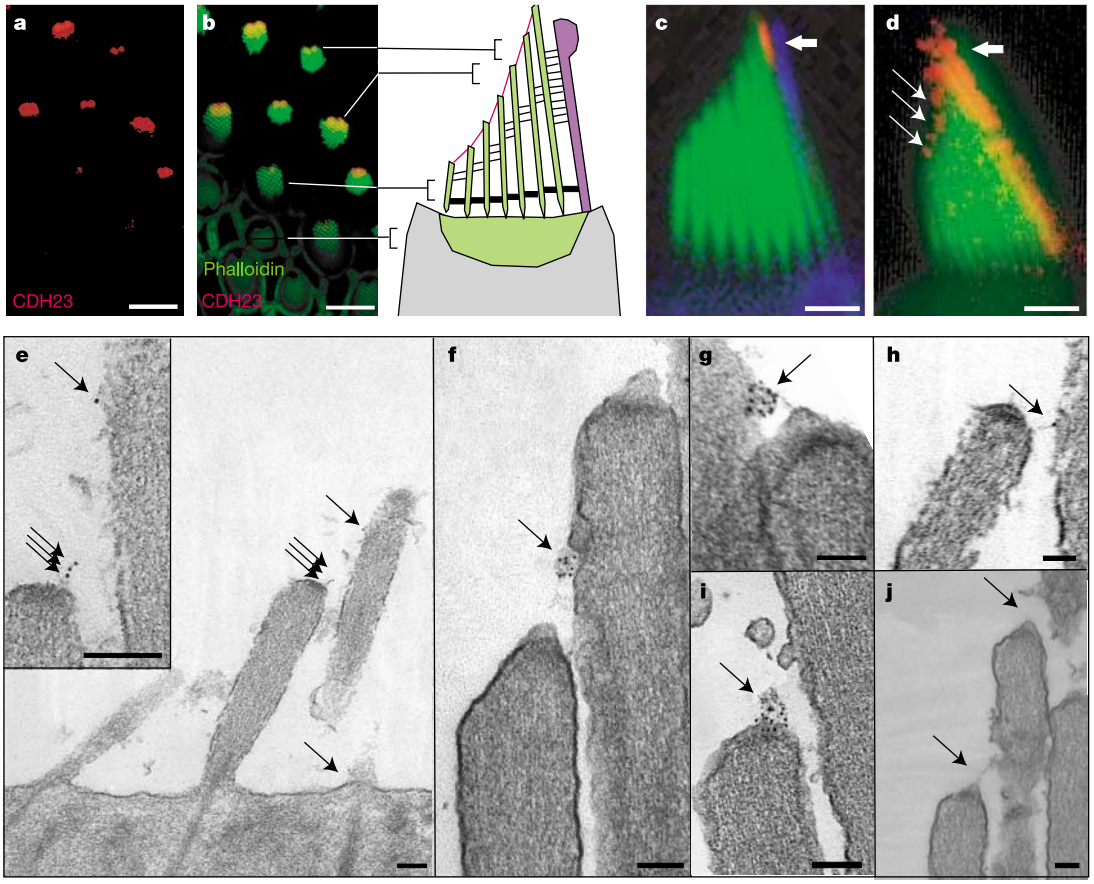

Figure 2 CDH23 expression in hair cells. **a**, **b**, Whole-mount bullfrog saccules were stained with CDH23*cyto antibody (red) and with phalloidin (green). Optical sections were cut through hair bundles at levels approximately as indicated. CDH23 was localized towards stereociliary tips. **c**, **d**, Isolated bullfrog hair cells were stained with anti-tubulin (blue) (**c**), and CDH23*cyto (red) and phalloidin (green) (**c**, **d**). In **c** the intensity gain was decreased during imaging to highlight CDH23 localization at the stereocilium–kinocilium interface (thick arrow). CDH23 was also localized at stereociliary tips (thin arrows). **e**–**j**, Immunogold electron microscopy in mouse (**e**) and bullfrog (**f**–**j**) hair cells; CDH23 was found at the tip link (arrows indicate localization of all gold particles in image). **j**, Primary antibody was omitted (arrows point to tip link). Scale bars: **a**, **b**, 11 μm; **c**, **d**, 5 μm; **e**–**j**, 100 nm.

contrast, CDH23*68 detected CDH23(+68) only in the hair bundle (Fig. 1f). At P42, when hair cells are mature and have lost their kinocilium, CDH23 was still expressed in cochlear hair cells, but only near stereociliary tips (Fig. 1i). In vestibular hair cells, which reach maturity around birth, CDH23 was confined by P5 to stereociliary tips (Fig. 1k). No CDH23 immunoreactivity was observed in *Cdh23*-deficient *waltzer* mice (Fig. 1d, j).

The CDH23*cyto antiserum cross-reacted with bullfrog CDH23 (Supplementary Fig. 2), allowing the analysis of CDH23 expression in bullfrog hair cells, which are larger than mouse hair cells and do not lose their kinocilium. Optical sections, oriented perpendicular to the hair bundle, revealed that CDH23 was concentrated near stereociliary tips (Fig. 2a, b). In isolated hair cells, CDH23 was concentrated where the tallest stereocilia contact the kinocilium and at stereociliary tips (Fig. 2c, d).

To test further whether CDH23 is a tip link component, we used immunoelectron microscopy with the same CDH23*cyto antibody that specifically labelled stereociliary tips in wild-type but not in *waltzer* mice as analysed by immunofluorescence microscopy (Fig. 1i–k). The antibody labelled the tip link in mouse and bullfrog hair cells (Fig. 2e–i). More than half (57%) of all gold particles ($n = 192$) were found at stereociliary tips, where the lower end of the tip link is expected to insert into stereocilia. The position of the side plaque marking the upper end of each tip link can be inferred from the position of the shorter adjacent stereocilium, and is several hundred nanometres higher (see Methods); 23% of the gold particles were detected in this position. Ten per cent of the gold particles were distributed randomly along stereocilia, and 10% were located outside stereocilia. We observed immunogold labelling intracellularly at tip link insertion points and extracellularly close to the plasma membrane. The length of the two-antibody sandwich (approximately 20–30 nm) and membrane rupture at tip links[15–17] might account for the apparent extracellular localization of gold particles. We observed similar extracellular immunogold localization when detecting the membrane phospholipid phosphatidylinositol-4,5-biphosphate in hair bundles (data not shown). We observed between 1 and 12 gold particles at tip link insertion sites: several gold particles were probably observed because more than one CDH23 molecule may be present; furthermore, the antibody is expected to recognize several epitopes within the ~268-amino-acid cytoplasmic domain of CDH23. No labelling was observed with secondary antibody alone (Fig. 2j). In bullfrog, CDH23*cyto also labelled kinociliary links (Supplementary Fig. 3; gold particles excluded from quantification).

The tip link is disrupted on exposure of hair cells to Ca^{2+} chelators and La^{3+} (refs 10, 18). Treatment of hair cells with EGTA (Fig. 3a–d) or BAPTA (data not shown) abolished bundle staining of CDH23 in approximately 75% of the hair cells. Instead, intense staining was observed in the pericuticular necklace (Fig. 3b), a vesicle-rich compartment at the apical hair-cell surface[19]. This CDH23 pool could arise from new synthesis, redistribution from the soma, or redistribution from stereocilia. In bundles that retained immunoreactivity, labelling in stereocilia was usually distributed more longitudinally than in controls (data not shown), supporting the latter hypothesis. Tip links reappear 12–24 h after removal of Ca^{2+} chelators[20]; similarly, we detected robust CDH23 immunoreactivity 24 h after removal of EGTA or BAPTA (Fig. 3d). Finally, treatment with La^{3+} not only disrupted the tip link but also caused immediate loss of CDH23 immunoreactivity from stereocilia. In contrast to results with Ca^{2+} chelators, no elevated

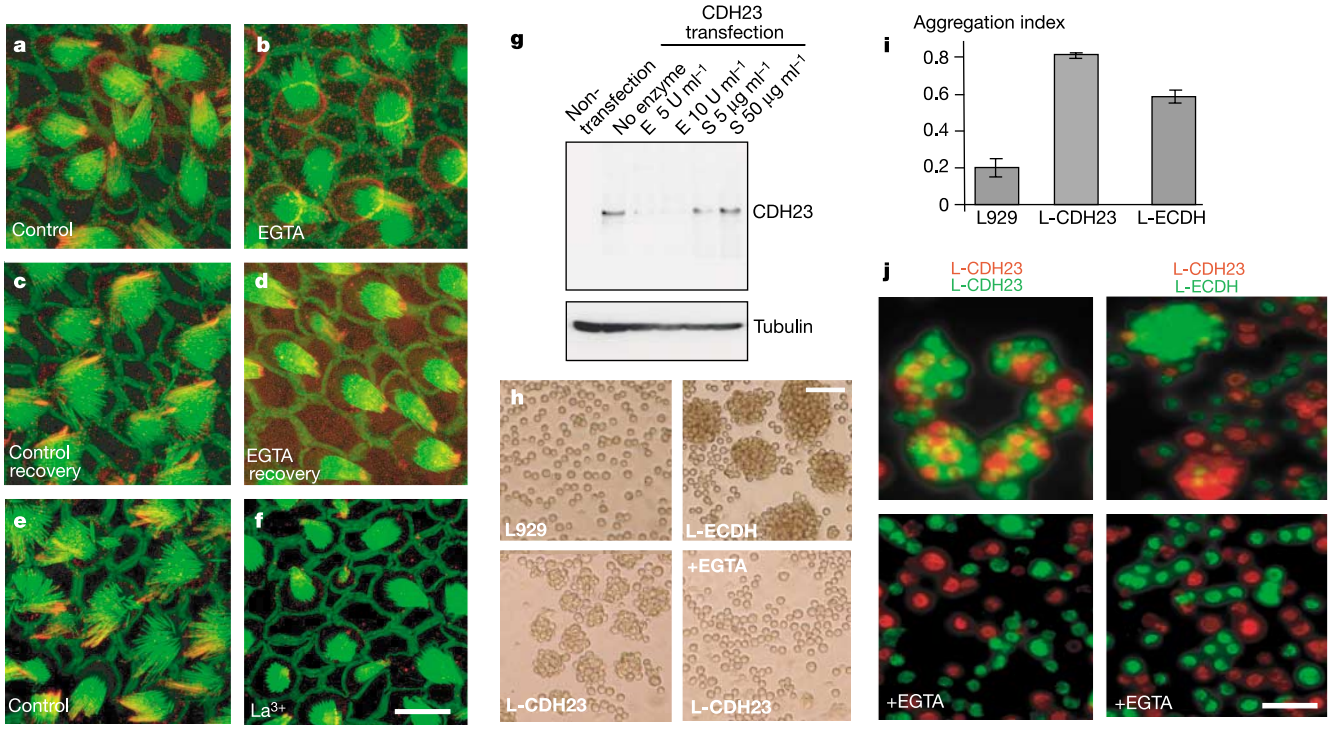

Figure 3 Biochemical properties of CDH23. **a**–**d**, Bullfrog saccules were treated with EGTA and stained with CDH23*cyto (red) and phalloidin (green). After EGTA treatment, CDH23 disappeared from stereocilia and appeared at the apical hair-cell surface; on EGTA removal, CDH23 reappeared in the bundle after 24 h (recovery). **e**, **f**, La^{3+} treatment caused loss of CDH23 immunostaining. **g**, Recombinant CDH23 protein expressed in HEK293 cells was sensitive to elastase (E) but not subtilisin (S). Control tubulin protein was insensitive to both proteases. **h**–**j**, Cell aggregation assays. **h**, L-CDH23 and L-ECDH cells formed aggregates. L-CDH23 aggregates were disrupted by EGTA. **i**, The aggregation index was determined[28] ($N_0 - N_T/N_0$; where N_0 is the number of particles with EGTA and N_T is the number of particles without EGTA). Mean and standard deviation are shown. **j**, DiI-labelled L-CDH23 cells (red) formed mixed aggregates with DiO-labelled L-CDH23 cells (green), but not with L-ECDH cells (green). Aggregation was blocked by EGTA. Scale bars: **a**–**f**, 8 μm; **h**, **j**, 60 μm.

pericuticular necklace labelling was observed after treatment with La^{3+} (Fig. 3e, f).

The tip link is sensitive to proteolytic digestion by elastase, but not by subtilisin, which cleaves ankle links[21,22]. We expressed the full-length CDH23 mRNA in HEK293 cells, treated them with elastase and subtilisin, and detected CDH23 by western blotting. CDH23 was degraded by elastase, but not by subtilisin (Fig. 3g).

CDH23 may connect stereocilia by a homophilic binding mechanism. To test CDH23 adhesive function, we established L929 cell lines expressing full-length CDH23 (L-CDH23 cells) or, as a control, E-cadherin (L-ECDH cells) (Supplementary Fig. 4). In cell aggregation assays, L-ECDH cells and L-CDH23 cells, but not parental L929 cells, formed aggregates; aggregation was inhibited by EGTA (Fig. 3h, i). Because aggregation of L-CDH23 cells might be mediated by homophilic interactions between CDH23 molecules or by heterophilic interactions with another cell surface receptor, we labelled cell lines with the fluorescence dyes DiI and DiO, and analysed aggregate formation by immunofluorescence microscopy. DiI-labelled L-CDH23 cells formed mixed aggregates with DiO-labelled L-CDH23 cells, but not with parental L929 cells or with L-ECDH cells (Fig. 3j). L-CDH23 and L-ECDH cells segregated into separate aggregates (Fig. 3j), whereas parental L929 cells remained as single cells (data not shown). These findings demonstrate that CDH23 mediates Ca^{2+}-dependent, homophilic cell adhesion.

Myosin-1c (MYO1C) is localized at stereociliary tips[23] and acts as an adaptation motor for the mechanotransduction channel[8]. To test whether MYO1C and CDH23 can interact directly or indirectly, we coexpressed in HEK293 cells MYO1C and a fusion protein containing the cytoplasmic domain of CDH23 and the transmembrane and extracellular domains of the interleukin-2 receptor (IL2R)[14] (Fig. 4a). As a control, we expressed a construct lacking the CDH23 cytoplasmic domain (IL2R–ΔCyto). All constructs were expressed efficiently (Fig. 4b, middle and bottom panels). MYO1C co-precipitated with IL2R–CDH23(−68) and IL2R–CDH23(+68), but not with IL2R–ΔCyto (Fig. 4b, top panel). Similarly, IL2R–CDH23(+68), but not IL2R–ΔCyto, co-precipitated with MYO1C (Fig. 4c). Using immunofluorescence microscopy of transfected cells (Fig. 4d; see also Supplementary Fig. 5), we found that both molecules co-localized at the cell periphery. Co-localization was dependent on the CHD23 cytoplasmic domain.

We provide here six lines of evidence supporting the proposal that CDH23 is a tip link component. First, CDH23 localizes at tip links. Second, CDH23 localizes to kinociliary links, which are immunologically related to tip links[11]. Third, reagents that disrupt tip link integrity, such as La^{3+} and EGTA[10,18], perturb CDH23 subcellular distribution in hair cells. Fourth, elastase disrupts the tip link[21] and cleaves CDH23 protein, whereas both tip links and CDH23 resist subtilisin proteolysis, which is known to cleave the ankle link[22]. Fifth, CDH23 mediates homophilic interactions, and Ca^{2+} chelators that disrupt the tip link disrupt CDH23 adhesive function. Sixth, CDH23 co-immunoprecipitates with MYO1C, the motor for slow adaptation of the mechanotransduction channel that is localized near stereociliary tips[8]. In agreement with our findings, tip links are absent in zebrafish that carry a mutation in the *cdh23* gene[24]. Our findings suggest an explanation of why CDH23 expression was not previously detected in mouse hair cells after P30 (ref. 25); that is, the kinocilium is not maintained in adult mouse

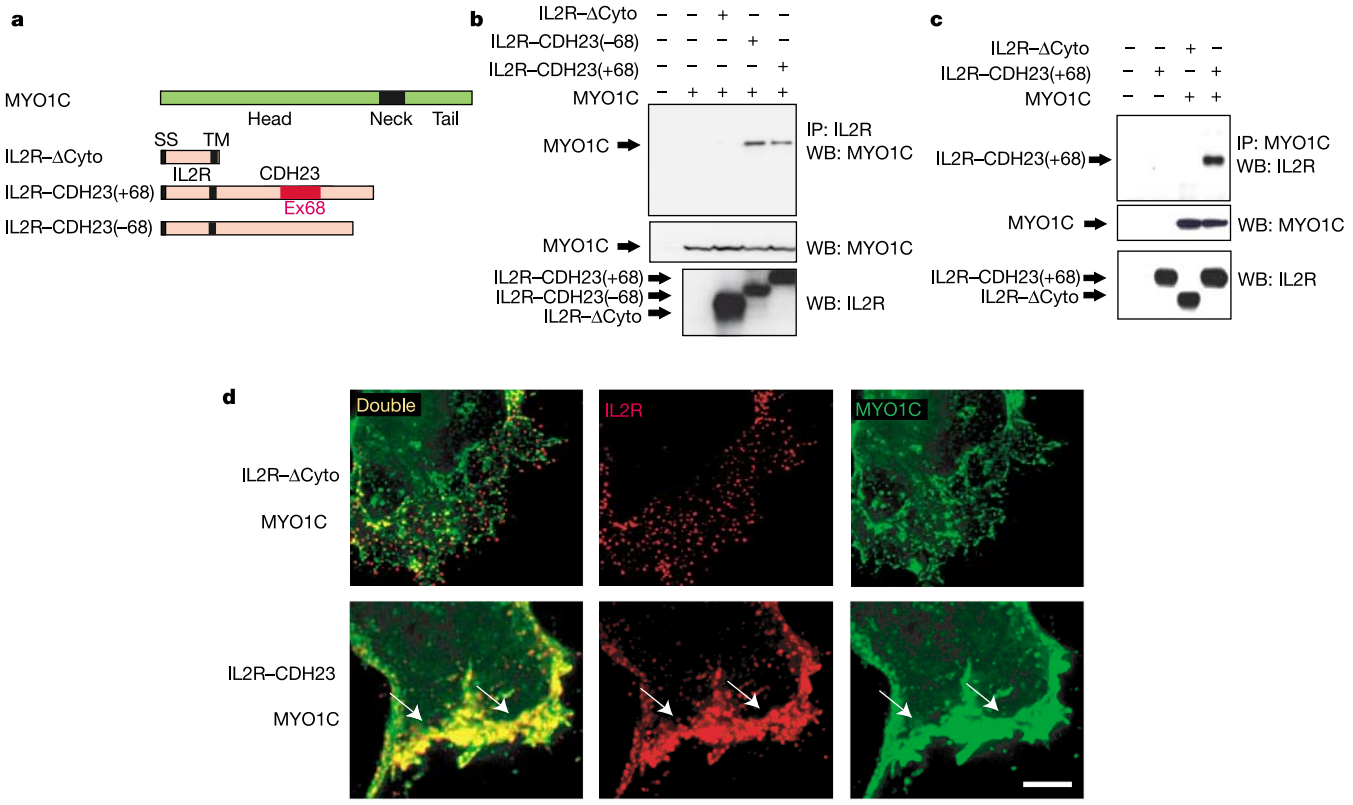

Figure 4 Interaction of IL2R–CDH23 with MYO1C. **a**, Diagram of MYO1C and of fusion proteins containing the extracellular and transmembrane domain of IL2R and the cytoplasmic domain of CDH23. **b**, Extracts from HEK293 cells transfected to express the constructs indicated on top of the panel were immunoprecipitated (IP) with IL2R or MYO1C antibodies. Proteins were visualized by western blotting (WB). As expression control, extracts were analysed without immunoprecipitation. **c**, MYO1C co-precipitated with IL2R–CDH23(−68) and IL2R–CDH23(+68), but not with IL2R–ΔCyto. **c**, IL2R–CDH23(+68) but not IL2R–ΔCyto co-immunoprecipitated with MYO1C. **d**, Transfected cells were stained with IL2R (red) and MYO1C (green) antibodies. MYO1C co-localized with IL2R–CDH23(+68) but not with IL2R-ΔCyto. Scale bar: 3.5 μm.

hair cells, and low expression at stereociliary tips may have prevented detection.

Our data are consistent with a model where CDH23 connects stereociliary tips, possibly by a homophilic binding mechanism. Because the tip link forks into two strands at its upper end and is larger in diameter than a cadherin dimer[18], the tip link is probably constructed of more than one CDH23 homophilic dimer. It may contain additional molecules such as the tip link antigen[11], which could engage in heterophilic interactions with CDH23. Because adaptation requires >50 MYO1C molecules per tip link[26] and the transduction channel must be in series between the tip link and motor complex, MYO1C and CDH23 probably interact in hair cells and in tissue culture cells through intermediate molecules. Although CDH23 has been shown to have a role in the maintenance of hair bundles during development[3], our findings suggest that its role in adult hair cells is to form kinocilia links and tip links, which transmit force to mechanically gated ion channels. A dual function for CDH23 in developing and adult hair cells could explain the phenotypic variability caused by mutations in the *Cdh23* gene. Mutations that affect assembly and maintenance of hair bundles probably inactivate *Cdh23* function[3]. In contrast, age-related hearing loss is caused by polymorphisms in an exon that encodes part of the extracellular domain[6]. This mutation may reduce CDH23 adhesive function and affect transduction channel gating. □

Methods

Antibodies and immunohistochemistry

The method to prepare and purify CDH23*cyto has been described[14]. CDH23*68 was raised in rabbits against a glutathione *S*-transferase (GST) fusion protein containing amino acids 3,133–3,291 of CDH23. The antiserum was affinity purified against a peptide with the amino acid sequence encoded by exon 68. Additional reagents were: anti-IL2R antibody (UBI), anti-MYO1C[23] and anti-tubulin antibody (Sigma), anti-E-cadherin antibody (Transduction Labs), and fluorescein isothiocyanate–phalloidin (Molecular Probes). Immunohistochemistry was carried out as described[14,19]. For staining of whole mounts, bullfrog sacculi were isolated in low Ca^{2+} saline (10 mM HEPES pH 7.4, 3 mM D-glucose, 2 mM $MgCl_2$, 2 mM KCl, 110 mM NaCl, 0.1 mM $CaCl_2$) and, where indicated, treated for 15–20 min with 5 mM La^{3+}, EGTA or BAPTA. For recovery, sacculi were incubated for 24 h at 18 °C in 80% MEM (GibcoBRL) containing 25 mM HEPES.

Immunogold electron microscopy

Tissues (6–8-week-old mice and adult bullfrogs) were fixed in 3.7% formaldehyde, 0.025% glutaraldehyde in 0.1 M phosphate buffer pH 7.4 for 1 h at room temperature, washed with 150 mM NaCl and 10 mM Tris-HCl, pH 7.4 (TBS), blocked in TBS containing 10% horse serum and 0.05% Tween 20 (TBS/HS), and incubated with CDH23*cyto antibody in TBS/HS overnight at 4 °C. Samples were incubated with 5 nm gold anti-rabbit antibody (Amersham) in TBS/HS, 1 mM sodium azide at 4 °C for 48–72 h, and post-fixed for 1 h with 2.5% glutaraldehyde in 0.1 M sodium cacodylate buffer pH 7.4. Samples were fixed for 1 h in 1% osmium tetroxide, dehydrated, embedded in Epon resin, and 50–75-nm sections were cut, placed on copper grids, stained for 1 h with 2% uranyl acetate in 50% ethanol for 45 min with lead citrate, and imaged in a Philips EM 208 microscope. The procedure produces good gold labelling, but tip links are less apparent[27]. The position of the side plaque marking the upper tip link end can be inferred from the position of the shorter adjacent stereocilium. The side plaque should be higher on the adjacent stereocilium by $d\sin\theta$, where d is tip link length (150–200 nm) and θ is the angle it forms relative to the tip of the short stereocilium (approximately 60°). The plaque can move up by 50–100 nm if tip links break[28], and the membrane at the shorter stereocilium can be tented upwards by >25 nm[10]. We looked for gold particles associated with stereocilia tips, and at a level 100–300 nm higher than the tip of the shorter adjacent stereocilium. Gold particles were also counted elsewhere along stereocilia and on sections outside hair cells and at the apical hair-cell surface.

Complementary DNA clones

CDH23 was cloned by RT–PCR from mouse vestibular RA. A 5′- and 3′-fragment was amplified (primers: 5′-ACCATGAGGTACTCCCTGGTCACA-3′, 5′-GCCAGGAATGTCCACACTCTGG-3′; and 5′-GAATGACATCAATGACAATGTGCC-3′, 5′-AAAGCTTTCACAGCTCCGTGATTTCCAGAGG-3′). During amplification, a *Hind*III site was introduced after the CDH23 stop codon. The fragments were cloned into pCRbluntII (Invitrogen). *Eco*RI–*Aat*II and *Aat*II–*Hind*III sites were used to clone the fragments into pcDNA3.1 (Invitrogen). Mouse MYO1C cDNA was amplified from IMAGE clone 5344331 (primers: 5′-ATAAGCTTACCATGGAGAGCGCCTTGACTG-3′, 5′-ATGAGATCCTCACCGAGAATTCAGCCGTGG-3′) and cloned into the *Hind*III–*Bam*HI site of pcDNA3.1. The IL2R–ΔCyto, IL2R–CDH23(+68) and IL2R–CDH23(−68) constructs have been described[14].

Cell aggregation assays

L929 cells were transfected with pSV2neo (ATCC) and expression vectors for E-cadherin or CDH23. Clones were selected in 500 μg ml^{-1} G418 (GibcoBRL) and analysed by western blotting. One CDH23-expressing clone was enriched by fluorescence-activated cell sorting. For cell aggregation assays, cells were trypsinized in HBSS containing 0.05% trypsin and 0.02% EDTA; soybean trypsin inhibitor (Sigma) was added to 0.05%, the cells were triturated, washed with MEMα medium (GibcoBRL) containing 10% horse serum, and re-suspended in the same medium supplemented with 50 μg ml^{-1} DNase I (Roche) and 25 mM HEPES, pH 7.4. Cells (1×10^5) were seeded in 0.5 ml medium into 24-well plates and rotated at 100 rotations per minute at 37 °C for 24 h. Where indicated, EGTA was added to 3 mM. Cells were fixed with 200 μl 25% glutaraldehyde. The aggregate number was quantified with a Coulter Counter[29]. Where indicated, cells were labelled with DiI or DiO (Molecular Probes).

Immunoprecipitation and immunocytochemistry

HEK293 cells were transfected with 1 μg DNA of each plasmid. After 24–36 h, extracts were prepared in RIPA buffer (50 mM Tris pH 7.4, 150 mM NaCl, 1% NP40, 0.5% deoxycholate, 0.1% SDS, 1 mM phenylmethylsulphonyl fluoride and 10 μg ml^{-1} aprotinin) and used for western blotting or immunoprecipitation[14]. For protease treatment, transfected HEK293 cells were washed with HBSS containing 10 mM HEPES (HHBSS) and treated with elastase or subtilisin (both Sigma) for 10 min at room temperature. Cells were washed on ice with HHBSS containing 2 mM PMSF and a protease inhibitor cocktail (Roche), lysed in 50 mM HEPES, pH 7.4, 150 mM NaCl, 1.5 mM $MgCl_2$, 1 mM $CaCl_2$, 10% (vol/vol) glycerol, 1% Triton and protease inhibitor cocktail, and analysed by western blotting. Immunocytochemistry was carried out as described[19].

Received 12 December 2003; accepted 9 March 2004; doi:10.1038/nature02483.
Published online 31 March 2004.

1. Müller, U. & Evans, A. L. Mechanisms that regulate mechanosensory hair cell differentiation. *Trends Cell Biol.* **11,** 334–342 (2001).
2. Gillespie, P. G. & Walker, R. G. Molecular basis of mechanosensory transduction. *Nature* **413,** 194–202 (2001).
3. Di Palma, F. *et al.* Mutations in *Cdh23*, encoding a new type of cadherin, cause stereocilia disorganization in *waltzer*, the mouse model for Usher syndrome type 1D. *Nature Genet.* **27,** 103–107 (2001).
4. Bolz, H. *et al.* Mutation of *CDH23*, encoding a new member of the cadherin gene family, causes Usher syndrome type 1D. *Nature Genet.* **27,** 108–112 (2001).
5. Bork, J. M. *et al.* Usher syndrome 1D and nonsyndromic autosomal recessive deafness DFNB12 are caused by allelic mutations of the novel cadherin-like gene CDH23. *Am. J. Hum. Genet.* **68,** 26–37 (2001).
6. Noben-Trauth, K., Zheng, Q. Y. & Johnson, K. R. Association of cadherin 23 with polygenic inheritance and genetic modification of sensorineural hearing loss. *Nature Genet.* **35,** 21–23 (2003).
7. Pickles, J. O., Comis, S. D. & Osborne, M. P. Cross-links between stereocilia in the guinea pig organ of Corti, and their possible relation to sensory transduction. *Hear. Res.* **15,** 103–112 (1984).
8. Holt, J. R. *et al.* A chemical-genetic strategy implicates myosin-1c in adaptation by hair cells. *Cell* **108,** 371–381 (2002).
9. Corey, D. P. & Hudspeth, A. J. Kinetics of the receptor current in bullfrog saccular hair cells. *J. Neurosci.* **3,** 962–976 (1983).
10. Assad, J. A., Shepherd, G. M. & Corey, D. P. Tip-link integrity and mechanical transduction in vertebrate hair cells. *Neuron* **7,** 985–994 (1991).
11. Goodyear, R. J. & Richardson, G. P. A novel antigen sensitive to calcium chelation that is associated with the tip links and kinocilial links of sensory hair bundles. *J. Neurosci.* **23,** 4878–4887 (2003).
12. Takeichi, M. Cadherins: a molecular family important in selective cell–cell adhesion. *Annu. Rev. Biochem.* **59,** 237–252 (1990).
13. Boggon, T. J. *et al.* C-cadherin ectodomain structure and implications for cell adhesion mechanisms. *Science* **296,** 1308–1313 (2002).
14. Siemens, J. *et al.* The Usher syndrome proteins cadherin 23 and harmonin form a complex by means of PDZ-domain interactions. *Proc. Natl Acad. Sci. USA* **99,** 14946–14951 (2002).
15. Little, K. F. & Neugebauer, C. D. Interconnections between the stereovilli of the fish inner ear. II. Systematic investigation of saccular bundles from *Rutilus rutilus* (Teleostei). *Cell Tissue Res.* **242,** 427–432 (1985).
16. Pickles, J. O., Rouse, G. W. & von Perger, M. Morphological correlates of mechanotransduction in acousticolateral hair cells. *Scan. Microsc.* **5,** 1115–1128 (1991).
17. Furness, D. N., Karkanevatos, A., West, B. & Hackney, C. M. An immunogold investigation of the distribution of calmodulin in the apex of cochlear hair cells. *Hear. Res.* **173,** 10–20 (2002).
18. Kachar, B., Parakkal, M., Kurc, M., Zhao, Y. & Gillespie, P. G. High-resolution structure of hair-cell tip links. *Proc. Natl Acad. Sci. USA* **97,** 13336–13341 (2000).
19. Hasson, T. *et al.* Unconventional myosins in inner-ear sensory epithelia. *J. Cell Biol.* **137,** 1287–1307 (1997).
20. Zhao, Y., Yamoah, E. N. & Gillespie, P. G. Regeneration of broken tip links and restoration of mechanical transduction in hair cells. *Proc. Natl Acad. Sci. USA* **93,** 15469–15474 (1996).
21. Osborne, M. P. & Comis, S. D. Action of elastase, collagenase and other enzymes upon linkages between stereocilia in the guinea-pig cochlea. *Acta Otolaryngol. (Stockh.)* **110,** 37–45 (1990).
22. Goodyear, R. & Richardson, G. The ankle-link antigen: an epitope sensitive to calcium chelation associated with the hair-cell surface and the calycal processes of photoreceptors. *J. Neurosci.* **19,** 3761–3772 (1999).
23. Gillespie, P. G., Wagner, M. C. & Hudspeth, A. J. Identification of a 120 kd hair-bundle myosin located near stereociliary tips. *Neuron* **11,** 581–594 (1993).
24. Söllner, C. *et al.* Mutations in *cadherin 23* affect tip links in zebrafish sensory hair cells. *Nature* advance online publication 31 March 2004 (doi:10.1038/nature02484).
25. Boeda, B. *et al.* Myosin VIIa, harmonin and cadherin 23, three Usher I gene products that cooperate to shape the sensory hair cell bundle. *EMBO J.* **21,** 6689–6699 (2002).
26. Hudspeth, A. J. & Gillespie, P. G. Pulling springs to tune transduction: adaptation by hair cells. *Neuron* **12,** 1–9 (1994).
27. Garcia, J. A., Yee, A. G., Gillespie, P. G. & Corey, D. P. Localization of myosin-Iβ near both ends of tip links in frog saccular hair cells. *J. Neurosci.* **18,** 8637–8647 (1998).

28. Shepherd, G. M. G., Assad, J. A., Prarakkal, M., Kachar, B. & Corey, D. P. Movement of the tip-link attachment is correlated with adaptation in bullfrog saccular hair cells. *J. Gen. Physiol.* **98,** 25A (1991).
29. Nagafuchi, A. & Takeichi, M. Cell binding function of E-cadherin is regulated by the cytoplasmic domain. *EMBO J.* **7,** 3679–3684 (1988).

Supplementary Information accompanies the paper on **www.nature.com/nature**.

Acknowledgements We thank R. Kemler for E-cadherin clones; M. Senften for L929 cells expressing E-cadherin; T. Hasson, B. Ranscht and H. C. VanSteenhouse for technical advice; and A. Kralli, L. Stowers and A. Patapoutian for critical reading of the manuscript. J.S. was supported by a fellowship from the Boehringer Ingelheim Fonds; A.R. by a C. J. Martin Fellowship from the National Health and Medical Research Council (Australia). This work was supported by grants from the NIDCD and NEI (U.M, P.G.G. and D.S.W.).

Competing interests statement The authors declare that they have no competing financial interests.

Correspondence and requests for materials should be addressed to U.M. (umueller@scripps.edu).

Mutations in *cadherin 23* affect tip links in zebrafish sensory hair cells

Christian Söllner[1], Gerd-Jörg Rauch[2], Jan Siemens[4], Robert Geisler[2], Stephan C. Schuster[3], the Tübingen 2000 Screen Consortium*, Ulrich Müller[4] & Teresa Nicolson[1,5]

[1]*Max-Planck-Institut für Entwicklungsbiologie, Spemannstrasse 35, 72076 Tübingen, Germany*
[2]*Abteilung Genetik,* [3]*AG Genomics & Signal transduction, Max-Planck-Institut für Entwicklungsbiologie, Spemannstrasse 35, 72076 Tübingen, Germany*
[4]*The Scripps Research Institute, 10550 N. Torrey Pines Road, Mail Drop ICND222, La Jolla, California 92037, USA*
[5]*Oregon Hearing Research Center and Vollum Institute, 3181 SW Sam Jackson Park Road, Portland, Oregon 97239, USA*

* A list of members of the Tübingen 2000 Screen Consortium and their affiliations appears at the end of the paper

Hair cells have highly organized bundles of apical projections, or stereocilia, that are deflected by sound and movement. Displacement of stereocilia stretches linkages at the tips of stereocilia that are thought to gate mechanosensory channels[1]. To identify the molecular machinery that mediates mechanotransduction in hair cells, zebrafish mutants were identified with defects in balance and hearing[2]. In *sputnik* mutants, stereociliary bundles are splayed to various degrees, with individuals displaying reduced or absent mechanotransduction[3,4]. Here we show that the defects in *sputnik* mutants are caused by mutations in *cadherin 23* (*cdh23*). Mutations in *Cdh23* also cause deafness and vestibular defects in mice and humans[5–9], and the protein is present in hair bundles[10,11]. We show that zebrafish Cdh23 protein is concentrated near the tips of hair bundles, and that tip links are absent in homozygous *sputnik*^{tc317e} larvae. Moreover, tip links are absent in larvae carrying weak alleles of *cdh23* that affect mechanotransduction but not hair bundle integrity. We conclude that Cdh23 is an essential tip link component required for hair-cell mechanotransduction.

Stereocilia are interconnected by extracellular filaments, and several linkages have been identified on the basis of their position along the bundle and sensitivity to proteases or calcium chelators[12–17]. These include ankle links near the base of the bundle, lateral links or shaft connectors in the medial part, and tip links near the stereociliary tips. Tip links are postulated to be a part of the mechanotransduction apparatus and are thought to physically tug open transducer channels when bundles are deflected in the excitatory direction[18]. The other links appear to make important structural contributions to bundle architecture and stiffness. Although some biochemical properties have been characterized[12–16], the molecular identity of these extracellular filaments is unknown. One exception is the lower lateral links, also called shaft connectors, which are absent in protein tyrosine phosphatase receptor Q knockout mice[17]. In addition, mutations that disrupt the integrity of hair-cell bundles in animal model organisms have identified unconventional myosins and novel cadherins as having a function in normal bundle formation and integrity[19,20].

In zebrafish, several auditory and vestibular mutants have been described with defects in bundle integrity[3,20]. Mutant *sputnik* larvae have splayed hair bundles and mechanotransduction is affected[3,4]. The recessive alleles of *sputnik* vary in strength, ranging from an obvious defect in bundle integrity and lack of extracellular receptor potentials to a fairly weak phenotype in which very few bundles are splayed and yet extracellular potentials are reduced by two-thirds.

To identify *sputnik*, we meiotically mapped the *sputnik* locus (allele *tj264a*), defining the critical interval by scoring over 2,500 homozygous mutant larvae with polymorphic markers (Fig. 1a). A chromosomal walk was initiated and a clone within the critical interval, PACc (BUSMP706A1551Q0), was shotgun sequenced (Fig. 1a). Four exons of *cdh23* were found on PACc and rapid amplification of cloned ends with polymerase chain reaction (RACE PCR) was used to generate the full-length sequence. Zebrafish *cdh23* encodes a 3,366 amino acid protein containing 27 ectodomains or extracellular repeats followed by a single transmembrane domain and a carboxy-terminal tail (Fig. 1b). The zebrafish Cdh23 protein is 68% identical and shares 81% similarity with the respective human and mouse CDH23 proteins[5–9]. Using PCR with reverse transcription (RT), we detected two additional splice variants of *cdh23* messenger RNA (Fig. 1b). Exon 68, which encodes a portion of the intracellular domain, is present only in the full-length form. We sequenced complementary DNAs from homozygous mutant larvae and detected nonsense and missense mutations, or insertions (Fig. 1b).

To determine where *cdh23* was expressed, we examined mRNA levels using *in situ* hybridization. mRNA was first detected in the embryonic ear at 24 h post-fertilization (h.p.f.) and at all later stages (Fig. 1c–e). The two patches of cells, which are clearly labelled at opposite ends of the otic vesicle, are the first hair cells to develop and express hair-cell-specific genes[20,21] (Fig. 1c). At later stages, *cdh23* mRNA was also detected in the brain, olfactory organ and in a subset of cells within the eye (data not shown). In the neuroepithelium of the ear and lateral line neuromasts, *cdh23* was expressed exclusively in hair cells (Fig. 1d, e). Hybridization with a sense probe did not yield a detectable signal (Supplementary Fig. 1).

In live, undissected *sputnik* larvae, detachment of bundles from kinocilia or splaying of stereocilia is visible, albeit at low resolution[3]. In order to assess the differences between the various alleles in *sputnik* larvae in more detail, we examined fluorescently labelled bundles in intact fixed larvae (Fig. 2). In larvae carrying a frameshift resulting in a nonsense mutation (*tc317e*), almost all (94%) of the bundles showed some splaying or were disorganized (Fig. 2b, i; $n = 48$ bundles). A similar percentage of bundles was also affected in *sputnik*^{t23576} larvae carrying a nonsense mutation (data not shown). Many bundles were splayed in *sputnik*^{tj264a} (74%) and *sputnik*^{tc242b} (59%) larvae, but intact bundles were also present (Fig. 2c, d, i; $n = 54$ and $n = 44$ bundles, respectively). It is worth noting that hair bundles treated with BAPTA exhibit severe splaying and have a broad, fan-like appearance[15], suggesting that the stronger alleles of *cdh23* do not cause complete splaying. Indeed, transmission electron microscopy (TEM) analysis suggests that the degree of splaying of stereocilia in *sputnik*^{tc317e} mutants is not severe (see Supplementary Fig. 2). In the weaker allele, *tz300a*, splaying was present (38%); however, over half of the bundles appeared to be unaffected and the degree of splaying was more subtle (Fig. 2e, i; $n = 39$ bundles). Finally, in larvae carrying the